

PDF hosted at the Radboud Repository of the Radboud University Nijmegen

The following full text is a publisher's version.

For additional information about this publication click this link.

<http://hdl.handle.net/2066/71986>

Please be advised that this information was generated on 2018-07-08 and may be subject to change.

Measurement of B_s^0 Mixing Parameters from the Flavor-Tagged Decay $B_s^0 \rightarrow J/\psi\phi$

V. M. Abazov,³⁶ B. Abbott,⁷⁵ M. Abolins,⁶⁵ B. S. Acharya,²⁹ M. Adams,⁵¹ T. Adams,⁴⁹ E. Aguilo,⁶ S. H. Ahn,³¹ M. Ahsan,⁵⁹ G. D. Alexeev,³⁶ G. Alkhazov,⁴⁰ A. Alton,^{64,*} G. Alverson,⁶³ G. A. Alves,² M. Anastasoae,³⁵ L. S. Ancu,³⁵ T. Andeen,⁵³ S. Anderson,⁴⁵ B. Andrieu,¹⁷ M. S. Anzels,⁵³ Y. Arnoud,¹⁴ M. Arov,⁶⁰ M. Arthaud,¹⁸ A. Askew,⁴⁹ B. Åsman,⁴¹ A. C. S. Assis Jesus,³ O. Atramentov,⁴⁹ C. Autermann,²¹ C. Avila,⁸ C. Ay,²⁴ F. Badaud,¹³ A. Baden,⁶¹ L. Bagby,⁵⁰ B. Baldin,⁵⁰ D. V. Bandurin,⁵⁹ P. Banerjee,²⁹ S. Banerjee,²⁹ E. Barberis,⁶³ A.-F. Barfuss,¹⁵ P. Bargassa,⁸⁰ P. Baringer,⁵⁸ J. Barreto,² J. F. Bartlett,⁵⁰ U. Bassler,¹⁸ D. Bauer,⁴³ S. Beale,⁶ A. Bean,⁵⁸ M. Begalli,³ M. Begel,⁷³ C. Belanger-Champagne,⁴¹ L. Bellantoni,⁵⁰ A. Bellavance,⁵⁰ J. A. Benitez,⁶⁵ S. B. Beri,²⁷ G. Bernardi,¹⁷ R. Bernhard,²³ I. Bertram,⁴² M. Bessaçon,¹⁸ R. Beuselinck,⁴³ V. A. Bezzubov,³⁹ P. C. Bhat,⁵⁰ V. Bhatnagar,²⁷ C. Biscarat,²⁰ G. Blazey,⁵² F. Blekman,⁴³ S. Blessing,⁴⁹ D. Bloch,¹⁹ K. Bloom,⁶⁷ A. Boehnlein,⁵⁰ D. Boline,⁶² T. A. Bolton,⁵⁹ G. Borissov,⁴² T. Bose,⁷⁷ A. Brandt,⁷⁸ R. Brock,⁶⁵ G. Brooijmans,⁷⁰ A. Bross,⁵⁰ D. Brown,⁸¹ N. J. Buchanan,⁴⁹ D. Buchholz,⁵³ M. Buehler,⁸¹ V. Buescher,²² V. Bunichev,³⁸ S. Burdin,^{42,†} S. Burke,⁴⁵ T. H. Burnett,⁸² C. P. Buszello,⁴³ J. M. Butler,⁶² P. Calfayan,²⁵ S. Calvet,¹⁶ J. Cammin,⁷¹ W. Carvalho,³ B. C. K. Casey,⁵⁰ H. Castilla-Valdez,³³ S. Chakrabarti,¹⁸ D. Chakraborty,⁵² K. Chan,⁶ K. M. Chan,⁵⁵ A. Chandra,⁴⁸ F. Charles,^{19,**} E. Cheu,⁴⁵ F. Chevallier,¹⁴ D. K. Cho,⁶² S. Choi,³² B. Choudhary,²⁸ L. Christofek,⁷⁷ T. Christoudias,⁴³ S. Cihangir,⁵⁰ D. Claes,⁶⁷ Y. Coadou,⁶ M. Cooke,⁸⁰ W. E. Cooper,⁵⁰ M. Corcoran,⁸⁰ F. Couderc,¹⁸ M.-C. Cousinou,¹⁵ S. Crépe-Renaudin,¹⁴ D. Cutts,⁷⁷ M. Ćwiok,³⁰ H. da Motta,² A. Das,⁴⁵ G. Davies,⁴³ K. De,⁷⁸ S. J. de Jong,³⁵ E. De La Cruz-Burelo,⁶⁴ C. De Oliveira Martins,³ J. D. Degenhardt,⁶⁴ F. Déliot,¹⁸ M. Demarteau,⁵⁰ R. Demina,⁷¹ D. Denisov,⁵⁰ S. P. Denisov,³⁹ S. Desai,⁵⁰ H. T. Diehl,⁵⁰ M. Diesburg,⁵⁰ A. Dominguez,⁶⁷ H. Dong,⁷² L. V. Dudko,³⁸ L. Duflot,¹⁶ S. R. Dugad,²⁹ D. Duggan,⁴⁹ A. Duperrin,¹⁵ J. Dyer,⁶⁵ A. Dyshkant,⁵² M. Eads,⁶⁷ D. Edmunds,⁶⁵ J. Ellison,⁴⁸ V. D. Elvira,⁵⁰ Y. Enari,⁷⁷ S. Eno,⁶¹ P. Ermolov,³⁸ H. Evans,⁵⁴ A. Evdokimov,⁷³ V. N. Evdokimov,³⁹ A. V. Ferapontov,⁵⁹ T. Ferbel,⁷¹ F. Fiedler,²⁴ F. Filthaut,³⁵ W. Fisher,⁵⁰ H. E. Fisk,⁵⁰ M. Ford,⁴⁴ M. Fortner,⁵² H. Fox,⁴² S. Fu,⁵⁰ S. Fuess,⁵⁰ T. Gadfort,⁷⁰ C. F. Galea,³⁵ E. Gallas,⁵⁰ C. Garcia,⁷¹ A. Garcia-Bellido,⁸² V. Gavrilov,³⁷ P. Gay,¹³ W. Geist,¹⁹ D. Gelé,¹⁹ C. E. Gerber,⁵¹ Y. Gershtein,⁴⁹ D. Gillberg,⁶ G. Ginther,⁷¹ N. Gollub,⁴¹ B. Gómez,⁸ A. Goussiou,⁸² P. D. Grannis,⁷² H. Greenlee,⁵⁰ Z. D. Greenwood,⁶⁰ E. M. Gregores,⁴ G. Grenier,²⁰ Ph. Gris,¹³ J.-F. Grivaz,¹⁶ A. Grohsjean,²⁵ S. Grünendahl,⁵⁰ M. W. Grünewald,³⁰ F. Guo,⁷² J. Guo,⁷² G. Gutierrez,⁵⁰ P. Gutierrez,⁷⁵ A. Haas,⁷⁰ N. J. Hadley,⁶¹ P. Haefner,²⁵ S. Hagopian,⁴⁹ J. Haley,⁶⁸ I. Hall,⁶⁵ R. E. Hall,⁴⁷ L. Han,⁷ K. Harder,⁴⁴ A. Harel,⁷¹ R. Harrington,⁶³ J. M. Hauptman,⁵⁷ R. Hauser,⁶⁵ J. Hays,⁴³ T. Hebbeker,²¹ D. Hedin,⁵² J. G. Hegeman,³⁴ J. M. Heinmiller,⁵¹ A. P. Heinson,⁴⁸ U. Heintz,⁶² C. Hensel,⁵⁸ K. Herner,⁷² G. Hesketh,⁶³ M. D. Hildreth,⁵⁵ R. Hirosky,⁸¹ J. D. Hobbs,⁷² B. Hoeneisen,¹² H. Hoeth,²⁶ M. Hohlfield,²² S. J. Hong,³¹ S. Hossain,⁷⁵ P. Houben,³⁴ Y. Hu,⁷² Z. Hubacek,¹⁰ V. Hynek,⁹ I. Iashvili,⁶⁹ R. Illingworth,⁵⁰ A. S. Ito,⁵⁰ S. Jabeen,⁶² M. Jaffré,¹⁶ S. Jain,⁷⁵ K. Jakobs,²³ C. Jarvis,⁶¹ R. Jesik,⁴³ K. Johns,⁴⁵ C. Johnson,⁷⁰ M. Johnson,⁵⁰ A. Jonckheere,⁵⁰ P. Jonsson,⁴³ A. Juste,⁵⁰ E. Kajfasz,¹⁵ A. M. Kalinin,³⁶ J. M. Kalk,⁶⁰ S. Kappler,²¹ D. Karmanov,³⁸ P. A. Kasper,⁵⁰ I. Katsanos,⁷⁰ D. Kau,⁴⁹ R. Kaur,²⁷ V. Kaushik,⁷⁸ R. Kehoe,⁷⁹ S. Kermiche,¹⁵ N. Khalatyan,⁵⁰ A. Khanov,⁷⁶ A. Kharchilava,⁶⁹ Y. M. Kharzheev,³⁶ D. Khatidze,⁷⁰ T. J. Kim,³¹ M. H. Kirby,⁵³ M. Kirsch,²¹ B. Klima,⁵⁰ J. M. Kohli,²⁷ J.-P. Konrath,²³ V. M. Korablev,³⁹ A. V. Kozelov,³⁹ J. Kraus,⁶⁵ D. Krop,⁵⁴ T. Kuhl,²⁴ A. Kumar,⁶⁹ A. Kupco,¹¹ T. Kurča,²⁰ J. Kvita,⁹ F. Lacroix,¹³ D. Lam,⁵⁵ S. Lammers,⁷⁰ G. Landsberg,⁷⁷ P. Lebrun,²⁰ W. M. Lee,⁵⁰ A. Leflat,³⁸ J. Lellouch,¹⁷ J. Leveque,⁴⁵ J. Li,⁷⁸ L. Li,⁴⁸ Q. Z. Li,⁵⁰ S. M. Lietti,⁵ J. G. R. Lima,⁵² D. Lincoln,⁵⁰ J. Linnemann,⁶⁵ V. V. Lipaev,³⁹ R. Lipton,⁵⁰ Y. Liu,⁷ Z. Liu,⁶ A. Lobodenko,⁴⁰ M. Lokajicek,¹¹ P. Love,⁴² H. J. Lubatti,⁸² R. Luna,³ A. L. Lyon,⁵⁰ A. K. A. Maciel,² D. Mackin,⁸⁰ R. J. Madaras,⁴⁶ P. Mättig,²⁶ C. Magass,²¹ A. Magerkurth,⁶⁴ P. K. Mal,⁵⁵ H. B. Malbouisson,³ S. Malik,⁶⁷ V. L. Malyshev,³⁶ H. S. Mao,⁵⁰ Y. Maravin,⁵⁹ B. Martin,¹⁴ R. McCarthy,⁷² A. Melnitchouk,⁶⁶ L. Mendoza,⁸ P. G. Mercadante,⁵ M. Merkin,³⁸ K. W. Merritt,⁵⁰ A. Meyer,²¹ J. Meyer,^{22,§} T. Millet,²⁰ J. Mitrevski,⁷⁰ J. Molina,³ R. K. Mommsen,⁴⁴ N. K. Mondal,²⁹ R. W. Moore,⁶ T. Moulík,⁵⁸ G. S. Muanza,²⁰ M. Mulders,⁵⁰ M. Mulhearn,⁷⁰ O. Mundal,²² L. Mundim,³ E. Nagy,¹⁵ M. Naimuddin,⁵⁰ M. Narain,⁷⁷ N. A. Naumann,³⁵ H. A. Neal,⁶⁴ J. P. Negret,⁸ P. Neustroev,⁴⁰ H. Nilsen,²³ H. Nogima,³ S. F. Novaes,⁵ T. Nunnemann,²⁵ V. O'Dell,⁵⁰ D. C. O'Neil,⁶ G. Obrant,⁴⁰ C. Ochando,¹⁶ D. Onoprienko,⁵⁹ N. Oshima,⁵⁰ N. Osman,⁴³ J. Osta,⁵⁵ R. Otec,¹⁰ G. J. Otero y Garzón,⁵⁰ M. Owen,⁴⁴ P. Padley,⁸⁰ M. Pangilinan,⁷⁷ N. Parashar,⁵⁶ S.-J. Park,⁷¹ S. K. Park,³¹ J. Parsons,⁷⁰ R. Partridge,⁷⁷ N. Parua,⁵⁴ A. Patwa,⁷³ G. Pawloski,⁸⁰ B. Penning,²³ M. Perfilov,³⁸ K. Peters,⁴⁴ Y. Peters,²⁶ P. Pétróff,¹⁶ M. Petteni,⁴³ R. Piegaia,¹ J. Piper,⁶⁵ M.-A. Pleier,²² P. L. M. Podesta-Lerma,^{33,‡} V. M. Podstavkov,⁵⁰ Y. Pogorelov,⁵⁵ M.-E. Pol,² P. Polozov,³⁷ B. G. Pope,⁶⁵ A. V. Popov,³⁹ C. Potter,⁶ W. L. Prado da Silva,³ H. B. Prosper,⁴⁹ S. Protopopescu,⁷³ J. Qian,⁶⁴ A. Quadt,^{22,§} B. Quinn,⁶⁶ A. Rakitine,⁴²

M. S. Rangel,² K. Ranjan,²⁸ P. N. Ratoff,⁴² P. Renkel,⁷⁹ S. Reucroft,⁶³ P. Rich,⁴⁴ J. Rieger,⁵⁴ M. Rijssenbeek,⁷² I. Ripp-Baudot,¹⁹ F. Rizatdinova,⁷⁶ S. Robinson,⁴³ R. F. Rodrigues,³ M. Rominsky,⁷⁵ C. Royon,¹⁸ P. Rubinov,⁵⁰ R. Ruchti,⁵⁵ G. Safronov,³⁷ G. Sajot,¹⁴ A. Sánchez-Hernández,³³ M. P. Sanders,¹⁷ A. Santoro,³ G. Savage,⁵⁰ L. Sawyer,⁶⁰ T. Scanlon,⁴³ D. Schaile,²⁵ R. D. Schamberger,⁷² Y. Scheglov,⁴⁰ H. Schellman,⁵³ T. Schliephake,²⁶ C. Schwanenberger,⁴⁴ A. Schwartzman,⁶⁸ R. Schwienhorst,⁶⁵ J. Sekaric,⁴⁹ H. Severini,⁷⁵ E. Shabalina,⁵¹ M. Shamim,⁵⁹ V. Shary,¹⁸ A. A. Shchukin,³⁹ R. K. Shivpuri,²⁸ V. Siccaldi,¹⁹ V. Simak,¹⁰ V. Sirotenko,⁵⁰ P. Skubic,⁷⁵ P. Slattery,⁷¹ D. Smirnov,⁵⁵ G. R. Snow,⁶⁷ J. Snow,⁷⁴ S. Snyder,⁷³ S. Söldner-Rembold,⁴⁴ L. Sonnenschein,¹⁷ A. Sopczak,⁴² M. Sosebee,⁷⁸ K. Soustruznik,⁹ B. Spurlock,⁷⁸ J. Stark,¹⁴ J. Steele,⁶⁰ V. Stolin,³⁷ D. A. Stoyanova,³⁹ J. Strandberg,⁶⁴ S. Strandberg,⁴¹ M. A. Strang,⁶⁹ E. Strauss,⁷² M. Strauss,⁷⁵ R. Ströhmer,²⁵ D. Strom,⁵³ L. Stutte,⁵⁰ S. Sumowidagdo,⁴⁹ P. Svoisky,⁵⁵ A. Sznajder,³ P. Tamburello,⁴⁵ A. Tanasijczuk,¹ W. Taylor,⁶ J. Temple,⁴⁵ B. Tiller,²⁵ F. Tissandier,¹³ M. Titov,¹⁸ V. V. Tokmenin,³⁶ T. Toole,⁶¹ I. Torchiani,²³ T. Trefzger,²⁴ D. Tsybychev,⁷² B. Tuchming,¹⁸ C. Tully,⁶⁸ P. M. Tuts,⁷⁰ R. Unalan,⁶⁵ L. Uvarov,⁴⁰ S. Uvarov,⁴⁰ S. Uzunyan,⁵² B. Vachon,⁶ P. J. van den Berg,³⁴ R. Van Kooten,⁵⁴ W. M. van Leeuwen,³⁴ N. Varelas,⁵¹ E. W. Varnes,⁴⁵ I. A. Vasilyev,³⁹ M. Vaupel,²⁶ P. Verdier,²⁰ L. S. Vertogradov,³⁶ M. Verzocchi,⁵⁰ F. Villeneuve-Seguié,⁴³ P. Vint,⁴³ P. Vokac,¹⁰ E. Von Toerne,⁵⁹ M. Voutilainen,⁶⁸ R. Wagner,⁶⁸ H. D. Wahl,⁴⁹ L. Wang,⁶¹ M. H. L. S. Wang,⁵⁰ J. Warchol,⁵⁵ G. Watts,⁸² M. Wayne,⁵⁵ G. Weber,²⁴ M. Weber,⁵⁰ L. Welty-Rieger,⁵⁴ A. Wenger,²³ N. Wermes,²² M. Wetstein,⁶¹ A. White,⁷⁸ D. Wicke,²⁶ G. W. Wilson,⁵⁸ S. J. Wimpenny,⁴⁸ M. Wobisch,⁶⁰ D. R. Wood,⁶³ T. R. Wyatt,⁴⁴ Y. Xie,⁷⁷ S. Yacoub,⁵³ R. Yamada,⁵⁰ M. Yan,⁶¹ T. Yasuda,⁵⁰ Y. A. Yatsunenko,³⁶ K. Yip,⁷³ H. D. Yoo,⁷⁷ S. W. Youn,⁵³ J. Yu,⁷⁸ A. Zatserklyaniy,⁵² C. Zeitnitz,²⁶ T. Zhao,⁸² B. Zhou,⁶⁴ J. Zhu,⁷² M. Zielinski,⁷¹ D. Zieminska,⁵⁴ A. Zieminski,^{54,*} L. Zivkovic,⁷⁰ V. Zutshi,⁵² and E. G. Zverev³⁸

(D0 Collaboration)

¹Universidad de Buenos Aires, Buenos Aires, Argentina²LAFEX, Centro Brasileiro de Pesquisas Físicas, Rio de Janeiro, Brazil³Universidade do Estado do Rio de Janeiro, Rio de Janeiro, Brazil⁴Universidade Federal do ABC, Santo André, Brazil⁵Instituto de Física Teórica, Universidade Estadual Paulista, São Paulo, Brazil⁶University of Alberta, Edmonton, Alberta, Canada,

Simon Fraser University, Burnaby, British Columbia, Canada,

York University, Toronto, Ontario, Canada,

and McGill University, Montreal, Quebec, Canada

⁷University of Science and Technology of China, Hefei, People's Republic of China⁸Universidad de los Andes, Bogotá, Colombia⁹Center for Particle Physics, Charles University, Prague, Czech Republic¹⁰Czech Technical University, Prague, Czech Republic¹¹Center for Particle Physics, Institute of Physics, Academy of Sciences of the Czech Republic, Prague, Czech Republic¹²Universidad San Francisco de Quito, Quito, Ecuador¹³LPC, Univ Blaise Pascal, CNRS/IN2P3, Clermont, France¹⁴LPSC, Université Joseph Fourier Grenoble 1, CNRS/IN2P3, Institut National Polytechnique de Grenoble, France¹⁵CPPM, IN2P3/CNRS, Université de la Méditerranée, Marseille, France¹⁶LAL, Univ Paris-Sud, IN2P3/CNRS, Orsay, France¹⁷LPNHE, IN2P3/CNRS, Universités Paris VI and VII, Paris, France¹⁸DAPNIA/Service de Physique des Particules, CEA, Saclay, France¹⁹IPHC, Université Louis Pasteur et Université de Haute Alsace, CNRS/IN2P3, Strasbourg, France²⁰IPNL, Université Lyon 1, CNRS/IN2P3, Villeurbanne, France and Université de Lyon, Lyon, France²¹III. Physikalisches Institut A, RWTH Aachen, Aachen, Germany²²Physikalisches Institut, Universität Bonn, Bonn, Germany²³Physikalisches Institut, Universität Freiburg, Freiburg, Germany²⁴Institut für Physik, Universität Mainz, Mainz, Germany²⁵Ludwig-Maximilians-Universität München, München, Germany²⁶Fachbereich Physik, University of Wuppertal, Wuppertal, Germany²⁷Panjab University, Chandigarh, India²⁸Delhi University, Delhi, India²⁹Tata Institute of Fundamental Research, Mumbai, India³⁰University College Dublin, Dublin, Ireland³¹Korea Detector Laboratory, Korea University, Seoul, Korea³²SungKyunKwan University, Suwon, Korea

- ³³CINVESTAV, Mexico City, Mexico
³⁴FOM-Institute NIKHEF and University of Amsterdam/NIKHEF, Amsterdam, The Netherlands
³⁵Radboud University Nijmegen/NIKHEF, Nijmegen, The Netherlands
³⁶Joint Institute for Nuclear Research, Dubna, Russia
³⁷Institute for Theoretical and Experimental Physics, Moscow, Russia
³⁸Moscow State University, Moscow, Russia
³⁹Institute for High Energy Physics, Protvino, Russia
⁴⁰Petersburg Nuclear Physics Institute, St. Petersburg, Russia
⁴¹Lund University, Lund, Sweden, Royal Institute of Technology and Stockholm University, Stockholm, Sweden, and Uppsala University, Uppsala, Sweden
⁴²Lancaster University, Lancaster, United Kingdom
⁴³Imperial College, London, United Kingdom
⁴⁴University of Manchester, Manchester, United Kingdom
⁴⁵University of Arizona, Tucson, Arizona 85721, USA
⁴⁶Lawrence Berkeley National Laboratory and University of California, Berkeley, California 94720, USA
⁴⁷California State University, Fresno, California 93740, USA
⁴⁸University of California, Riverside, California 92521, USA
⁴⁹Florida State University, Tallahassee, Florida 32306, USA
⁵⁰Fermi National Accelerator Laboratory, Batavia, Illinois 60510, USA
⁵¹University of Illinois at Chicago, Chicago, Illinois 60607, USA
⁵²Northern Illinois University, DeKalb, Illinois 60115, USA
⁵³Northwestern University, Evanston, Illinois 60208, USA
⁵⁴Indiana University, Bloomington, Indiana 47405, USA
⁵⁵University of Notre Dame, Notre Dame, Indiana 46556, USA
⁵⁶Purdue University Calumet, Hammond, Indiana 46323, USA
⁵⁷Iowa State University, Ames, Iowa 50011, USA
⁵⁸University of Kansas, Lawrence, Kansas 66045, USA
⁵⁹Kansas State University, Manhattan, Kansas 66506, USA
⁶⁰Louisiana Tech University, Ruston, Louisiana 71272, USA
⁶¹University of Maryland, College Park, Maryland 20742, USA
⁶²Boston University, Boston, Massachusetts 02215, USA
⁶³Northeastern University, Boston, Massachusetts 02115, USA
⁶⁴University of Michigan, Ann Arbor, Michigan 48109, USA
⁶⁵Michigan State University, East Lansing, Michigan 48824, USA
⁶⁶University of Mississippi, University, Mississippi 38677, USA
⁶⁷University of Nebraska, Lincoln, Nebraska 68588, USA
⁶⁸Princeton University, Princeton, New Jersey 08544, USA
⁶⁹State University of New York, Buffalo, New York 14260, USA
⁷⁰Columbia University, New York, New York 10027, USA
⁷¹University of Rochester, Rochester, New York 14627, USA
⁷²State University of New York, Stony Brook, New York 11794, USA
⁷³Brookhaven National Laboratory, Upton, New York 11973, USA
⁷⁴Langston University, Langston, Oklahoma 73050, USA
⁷⁵University of Oklahoma, Norman, Oklahoma 73019, USA
⁷⁶Oklahoma State University, Stillwater, Oklahoma 74078, USA
⁷⁷Brown University, Providence, Rhode Island 02912, USA
⁷⁸University of Texas, Arlington, Texas 76019, USA
⁷⁹Southern Methodist University, Dallas, Texas 75275, USA
⁸⁰Rice University, Houston, Texas 77005, USA
⁸¹University of Virginia, Charlottesville, Virginia 22901, USA
⁸²University of Washington, Seattle, Washington 98195, USA

(Received 18 February 2008; revised manuscript received 20 October 2008; published 9 December 2008)

From an analysis of the flavor-tagged decay $B_s^0 \rightarrow J/\psi \phi$ we obtain the width difference between the B_s^0 light and heavy mass eigenstates, $\Delta\Gamma_s = 0.19 \pm 0.07(\text{stat})_{-0.01}^{+0.02}(\text{syst}) \text{ ps}^{-1}$, and the CP -violating phase, $\phi_s = -0.57_{-0.30}^{+0.24}(\text{stat})_{-0.02}^{+0.08}(\text{syst})$. The allowed 90% CL intervals of $\Delta\Gamma_s$ and ϕ_s are $0.06 < \Delta\Gamma_s < 0.30 \text{ ps}^{-1}$ and $-1.20 < \phi_s < 0.06$, respectively. The data sample corresponds to an integrated luminosity of 2.8 fb^{-1} accumulated with the D0 detector at the Fermilab Tevatron collider.

In the standard model (SM), the light (L) and heavy (H) mass eigenstates of the mixed B_s^0 system are expected to have sizeable mass and decay width differences: $\Delta M_s \equiv M_H - M_L$ and $\Delta \Gamma_s \equiv \Gamma_L - \Gamma_H$. The two mass eigenstates are expected to be almost pure CP eigenstates. The CP -violating mixing phase that appears in $b \rightarrow c\bar{c}s$ decays is predicted [1,2] to be $\phi_s = -2\beta_s = 2\arg[-V_{tb}V_{ts}^*/V_{cb}V_{cs}^*] = -0.038 \pm 0.002$, where V_{ij} are elements of the Cabibbo-Kobayashi-Maskawa quark-mixing matrix [3]. New phenomena may alter the phase to $\phi_s = -2\beta_s + \phi_s^\Delta$.

In Ref. [4], we presented an analysis of the decay chain $B_s^0 \rightarrow J/\psi \phi$, $J/\psi \rightarrow \mu^+ \mu^-$, $\phi \rightarrow K^+ K^-$ based on 1.1 fb^{-1} of data collected with the D0 detector [5] at the Fermilab Tevatron collider. In that analysis we measured $\Delta \Gamma_s$ and the average lifetime of the B_s^0 system, $\bar{\tau}_s = 1/\bar{\Gamma}_s$, where $\bar{\Gamma}_s \equiv (\Gamma_H + \Gamma_L)/2$. The CP -violating phase ϕ_s was also extracted for the first time. The measurement correlated two solutions for ϕ_s with two corresponding solutions for $\Delta \Gamma_s$. Improved precision was obtained by refitting the results using additional experimental constraints [6]. Here we present new D0 results of an analysis that includes information on the B_s^0 flavor at production time. Adding this information resolves the sign ambiguity on ϕ_s for a given $\Delta \Gamma_s$ and improves the precision of the measurement. The analysis is based on an increased data set, corresponding to an integrated luminosity of 2.8 fb^{-1} .

We reconstruct the decay chain $B_s^0 \rightarrow J/\psi \phi$, $J/\psi \rightarrow \mu^+ \mu^-$, $\phi \rightarrow K^+ K^-$ from candidate (J/ψ , ϕ) pairs consistent with coming from a common vertex and having an invariant mass in the range 5.0–5.8 GeV. The event selection follows that in Ref. [4]. The invariant mass distribution of the 48047 candidates is shown in Fig. 1. The curves are projections of the maximum likelihood fit, described below. The fit assigns 1967 ± 65 (stat) events to the B_s^0 decay. The flavor of the initial state of the B_s^0 candidate is determined by exploiting the properties of particles produced by the other b hadron (“opposite-side tagging”) and the properties of particles accompanying the B_s^0 meson (“same-side tagging”). The variables used to construct the opposite-side tagging are described in Ref. [7] where we applied the “flavor tagging” to separate B^0 and \bar{B}^0 decays. The only difference to the description in Ref. [7] is that the events that do not contain either the opposite lepton or the secondary vertex, and that were not used for the flavor tagging before, are now tagged with the event-charge variable defined in Ref. [7].

Same-side tagging is based on the sign of an associated charged kaon formed in the hadronization process. A $B_s^0(b\bar{s})$ meson is expected to be accompanied by a strange meson, e.g., $K^+(u\bar{s})$ meson that can be used for flavor tagging. Such a configuration is formed when the initial \bar{b} antiquark picks up an s quark from a virtual $s\bar{s}$ pair and the \bar{s} antiquark becomes a constituent of an accompanying K^+ meson. Candidates for the associated kaon are all

tracks with transverse momentum $p_T > 500 \text{ MeV}$ that are not used in the B_s^0 reconstruction. We define the quantity $\Delta R = \sqrt{(\Delta\phi)^2 + (\Delta\eta)^2}$, where $\Delta\phi$ ($\Delta\eta$) is the distance in the azimuthal angle (pseudorapidity) between the given track and the B_s meson, and select the track with the minimum value of ΔR . The corresponding discriminating variable for the flavor tagging is defined as the product of the particle charge and ΔR . Another discriminating variable is Q_{jet} , the p_T -weighted average of all track charges q_i within the cone $\cos[\angle(\vec{p}, \vec{p}_B)] > 0.8$ around the B meson: $Q_{\text{jet}} = [\sum_i q_i (p_T^i)^{0.6}] / [\sum_i (p_T^i)^{0.6}]$. The same tagging technique has been successfully applied in the measurement of the B_s^0 oscillation frequency [8].

The discriminating variables of both the same-side and opposite-side tagging are combined using the likelihood-ratio method described in Ref. [7]. The performance of the combined tagging is taken from a Monte Carlo (MC) simulation of the $B_s^0 \rightarrow J/\psi \phi$ process and is verified with the $B^\pm \rightarrow J/\psi K^\pm$ process for which we find the simulated tagging to be in agreement with data. The effective tagging power, as defined in Ref. [7], is $\mathcal{P} = (4.68 \pm 0.54)\%$. The purity of the flavor tag as a function of an over-all flavor discriminant is determined and parameterized, and the related probability $P(B_s)$ of having a pure state B_s^0 at $t = 0$ is used event-by-event in the fit described below.

We perform an unbinned maximum likelihood fit to the proper decay time, three decay angles characterizing the final state, and the mass of the B_s^0 candidate. The likelihood function \mathcal{L} is given by

$$\mathcal{L} = \prod_{i=1}^N [f_{\text{sig}} \mathcal{F}_{\text{sig}}^i + (1 - f_{\text{sig}}) \mathcal{F}_{\text{bck}}^i], \quad (1)$$

where N is the total number of events, and f_{sig} is the

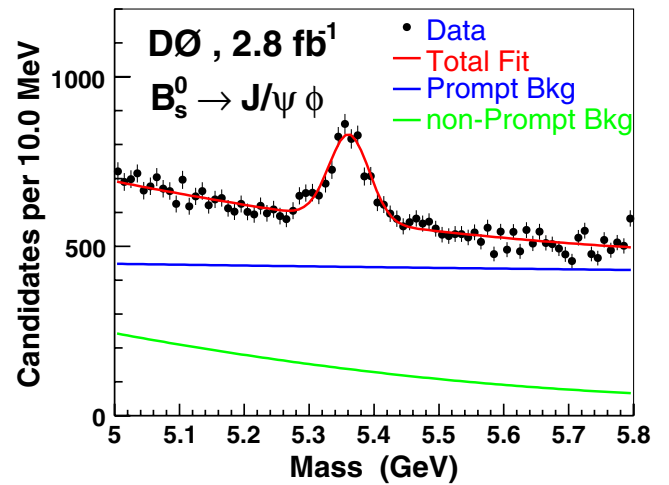


FIG. 1 (color online). The invariant mass distribution of the (J/ψ , ϕ) system for B_s^0 candidates. The curves are projections of the maximum likelihood fit (see text).

fraction of signal in the sample. The function $\mathcal{F}_{\text{sig}}^i$ describes the distribution of the signal in mass, proper decay time, and the decay angles. For the signal mass distribution, we use a Gaussian function with free mean and width. The proper decay time distribution of the L or H component of the signal is parametrized by an exponential convoluted with a Gaussian function. The width of the Gaussian is taken from the event-by-event estimate of the ct uncertainty $\sigma(\text{ct})$, scaled by an overall calibration factor determined from the fit to the prompt component of the background. $\mathcal{F}_{\text{bck}}^i$ is the product of the background mass, proper decay time, and angular probability density functions. Background is divided into two categories. “Prompt” background is due to directly produced J/ψ mesons accompanied by random tracks arising from ha-

dronization. This background is distinguished from “non-prompt” background, where the J/ψ meson is a product of a B -hadron decay while the tracks forming the ϕ candidate emanate from a multibody decay of a B hadron or from hadronization.

The decay amplitude of the B_s^0 and \bar{B}_s^0 mesons is decomposed into three independent components corresponding to linear polarization states of the vector mesons J/ψ and ϕ , which are either longitudinal (0) or transverse to their direction of motion, and parallel (\parallel) or perpendicular (\perp) to each other. The time evolution of the angular distribution of the decay products, expressed in terms of the magnitudes $|A_0|$, $|A_{\parallel}|$, and $|A_{\perp}|$, and two relative strong phases $\delta_1 = -\delta_{\parallel} + \delta_{\perp}$ and $\delta_2 = -\delta_0 + \delta_{\perp}$ of the amplitudes, is given in Refs. [9,10]:

$$\begin{aligned} \frac{d^4\Gamma}{dtd\cos\theta d\varphi d\cos\psi} &\propto 2\cos^2\psi(1 - \sin^2\theta\cos^2\varphi)|A_0(t)|^2 + \sin^2\psi(1 - \sin^2\theta\sin^2\varphi)|A_{\parallel}(t)|^2 + \sin^2\psi\sin^2\theta|A_{\perp}(t)|^2 \\ &+ (1/\sqrt{2})\sin 2\psi\sin^2\theta\sin 2\varphi\text{Re}(A_0^*(t)A_{\parallel}(t)) + (1/\sqrt{2})\sin 2\psi\sin 2\theta\cos\varphi\text{Im}(A_0^*(t)A_{\perp}(t)) \\ &- \sin^2\psi\sin 2\theta\sin\varphi\text{Im}(A_{\parallel}^*(t)A_{\perp}(t)). \end{aligned} \quad (2)$$

Polarization amplitudes for B_s^0 (upper sign) and \bar{B}_s^0 (lower sign) are given by the following equations:

$$|A_{0,\parallel}(t)|^2 = |A_{0,\parallel}(0)|^2[\mathcal{T}_{\pm} \pm e^{-\tilde{\Gamma}t}\sin\phi_s\sin(\Delta M_s t)], \quad |A_{\perp}(t)|^2 = |A_{\perp}(0)|^2[\mathcal{T}_{\pm} \mp e^{-\tilde{\Gamma}t}\sin\phi_s\sin(\Delta M_s t)],$$

$$\text{Re}(A_0^*(t)A_{\parallel}(t)) = |A_0(0)||A_{\parallel}(0)|\cos(\delta_2 - \delta_1) \times [\mathcal{T}_{\pm} \pm e^{-\tilde{\Gamma}t}\sin\phi_s\sin(\Delta M_s t)],$$

$$\begin{aligned} \text{Im}(A_0^*(t)A_{\perp}(t)) &= |A_0(0)||A_{\perp}(0)| \times [e^{-\tilde{\Gamma}t}(\pm\sin\delta_2\cos(\Delta M_s t) \mp \cos\delta_2\sin(\Delta M_s t)\cos\phi_s) \\ &- (1/2)(e^{-\Gamma_H t} - e^{-\Gamma_L t})\sin\phi_s\cos\delta_2], \end{aligned}$$

$$\begin{aligned} \text{Im}(A_{\parallel}^*(t)A_{\perp}(t)) &= |A_{\parallel}(0)||A_{\perp}(0)| \times [e^{-\tilde{\Gamma}t}(\pm\sin\delta_1\cos(\Delta M_s t) \mp \cos\delta_1\sin(\Delta M_s t)\cos\phi_s) \\ &- (1/2)(e^{-\Gamma_H t} - e^{-\Gamma_L t})\sin\phi_s\cos\delta_1], \end{aligned}$$

where $\mathcal{T}_{\pm} = (1/2)[(1 \pm \cos\phi_s)e^{-\Gamma_L t} + (1 \mp \cos\phi_s)e^{-\Gamma_H t}]$. For a given event, the decay rate is the sum of the B_s^0 and \bar{B}_s^0 rates weighted by $P(B_s)$ and $1 - P(B_s)$, respectively, and by the detector acceptance.

In the coordinate system of the J/ψ rest frame (where the ϕ meson moves in the x direction, the z axis is perpendicular to the decay plane of $\phi \rightarrow K^+K^-$, and $p_y(K^+) \geq 0$), the transversity polar and azimuthal angles (θ, φ) describe the direction of the μ^+ , and ψ is the angle between $\vec{p}(K^+)$ and $-\vec{p}(J/\psi)$ in the ϕ rest frame.

We model the acceptance and resolution of the three angles by fits using polynomial functions, with parameters determined using MC simulations. Events generated uniformly in the three-angle space were processed through the standard GEANT-based [11] simulation of the D0 detector, and reconstructed and selected as real data. Simulated events were reweighted to match the kinematic distributions observed in the data.

The proper decay time distribution shape of the background is described as a sum of a prompt component,

TABLE I. Summary of the likelihood fit results. The first column shows the results of the fit with a Gaussian constraint on δ_i . The second column shows two solutions with $\Delta\Gamma_s > 0$ yielded by the fit with free δ_i . Each of the two solutions has a mirror solution with $\Delta\Gamma_s < 0$ as explained in the text.

	δ_i constrained	δ_i free
$\bar{\tau}_s$ (ps)	1.52 ± 0.06	1.52 ± 0.06
$\Delta\Gamma_s$ (ps $^{-1}$)	0.19 ± 0.07	$0.20_{-0.08}^{+0.06}$
$A_{\perp}(0)$	0.41 ± 0.04	0.41 ± 0.04
$ A_0(0) ^2 - A_{\parallel}(0) ^2$	0.34 ± 0.05	0.34 ± 0.05
δ_1	-0.52 ± 0.42	$-0.18 \pm 0.90, 1.05 \pm 0.59$
$\delta_1 - \delta_2$	2.59 ± 0.29	$2.61 \pm 0.28, -2.61 \pm 0.29$
ϕ_s	$-0.57_{-0.30}^{+0.24}$	$-0.59_{-0.28}^{+0.31}$
ΔM_s (ps $^{-1}$)	$\equiv 17.77$	$\equiv 17.77$

TABLE II. Sources of systematic uncertainty in the results for the case of free ϕ_s .

Source	$\bar{\tau}_s$ (ps)	$\Delta\Gamma_s$ (ps $^{-1}$)	$A_{\perp}(0)$	$ A_0(0) ^2 - A_{\parallel}(0) ^2$	ϕ_s
Acceptance	± 0.003	± 0.003	± 0.005	± 0.03	± 0.005
Signal mass model	-0.01	$+0.006$	-0.003	-0.001	-0.006
Flavor purity estimate	± 0.001	± 0.001	± 0.001	± 0.001	± 0.01
Flavor purity model	$+0.003$	$+0.003$	<0.001	$+0.002$	$+0.04$
Background model	$+0.003$	$+0.02$	-0.02	-0.01	$+0.02$
ΔM_s input	± 0.01	± 0.001	± 0.001	± 0.001	$+0.06, -0.01$
Total	± 0.01	$+0.02, -0.01$	$+0.01, -0.02$	± 0.03	$+0.08, -0.02$

modeled as a Gaussian function centered at zero, and a nonprompt component. The nonprompt component is modeled as a superposition of one exponential for $t < 0$ and two exponentials for $t > 0$, with free slopes and normalizations. The distributions of the backgrounds in mass, $\cos\theta$, φ , and $\cos\psi$ are parametrized by low-order polynomials. We also allow for a background term analogous to the interference term of the A_0 and A_{\parallel} waves, with one free coefficient. For each of the above background functions we use two separate sets of free parameters for the prompt and nonprompt components.

In the following, we fix ΔM_s to 17.77 ± 0.12 ps $^{-1}$, as measured in Ref. [12]. The phases analogous to δ_i have been measured for the decay $B_d^0 \rightarrow J/\psi K^*$ at the B factories. We allow the phases δ_i to vary around the world-average values [13] for the $B_d^0 \rightarrow J/\psi K^*$ decay, $\delta_1 = -0.46$ and $\delta_2 = 2.92$, under a Gaussian constraint. The width of the Gaussian, chosen to be $\pi/5$, allows for some degree of violation of the $SU(3)$ symmetry relating the two decay processes, while still effectively constraining the signs of $\cos\delta_i$ to agree with those of Ref. [13]. The mirror solution with $\cos\delta_1 < 0$ is disfavored on theoretical [14] and experimental [15] grounds.

Results of the fit are presented in Table I. The fit yields a likelihood maximum at $\phi_s = -0.57^{+0.24}_{-0.30}$ and $\Delta\Gamma_s = 0.19 \pm 0.07$ ps $^{-1}$, where the errors are statistical only. Confidence-level contours in the $\phi_s - \Delta\Gamma_s$ plane are shown in Fig. 2. Studies using pseudoexperiments with similar statistical sensitivity indicate an expected statistical uncertainty in ϕ_s of 0.33 and no significant biases. The test finds allowed ranges at the 90% CL of $-1.20 < \phi_s < 0.06$ and $0.06 < \Delta\Gamma_s < 0.30$ ps $^{-1}$. To quantify the level of agreement with the SM, we use pseudoexperiments with the “true” value of the parameter ϕ_s set to $\phi_s = -2\beta_s (= -0.04)$ predicted by the SM. We find the probability of 6.6% to obtain a fitted value of ϕ_s lower than -0.57 . With this input ϕ_s , we obtain $\Delta\Gamma_s = 0.14 \pm 0.07$ ps $^{-1}$. This is consistent with the theoretical prediction of 0.088 ± 0.017 ps $^{-1}$ [1].

The fit results for the case of free δ_i are shown in the second column in Table I. The maximum likelihood occurs at two sets of phases δ_i . In addition, the signal probability distribution is invariant under the simultaneous transformation ($\Delta\Gamma_s \rightarrow -\Delta\Gamma_s$, $\phi_s \rightarrow \pi - \phi_s$, $\delta_1 \rightarrow \pi - \delta_1$,

$\delta_2 \rightarrow \pi - \delta_2$). There are two allowed ranges of ϕ_s and $\Delta\Gamma_s$ at the 90% CL, ($-1.22 < \phi_s < -0.08$, $0.05 < \Delta\Gamma_s < 0.33$ ps $^{-1}$), and ($-3.06 < \phi_s < -1.92$, $-0.33 < \Delta\Gamma_s < -0.05$ ps $^{-1}$). For the SM hypothesis, we find a probability of 8.5% to obtain a likelihood ratio higher than that observed in the data.

The measurement uncertainties are dominated by the limited statistics. Uncertainty in the acceptance as a function of the transversity angles is small, the largest effect is on $|A_0(0)|^2 - |A_{\parallel}(0)|^2$. Effects of the imperfect knowledge of the flavor-tagging purity are estimated by varying the flavor purity parametrization within uncertainties. The likelihood definition does not include the differences between the distributions of the flavor-tagging probability for various components of the sample. We find the effect of adding this dependence small, and assign an appropriate systematic uncertainty. The “interference” term in the background model accounts for the collective effect of various physics processes. However, its presence may be partially due to detector acceptance effects. Therefore, we

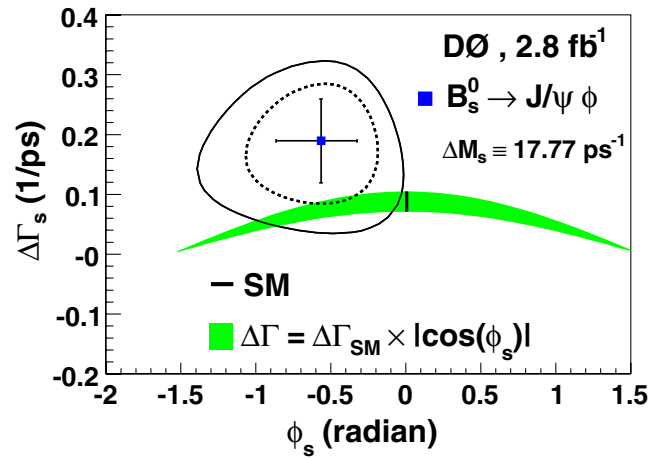


FIG. 2 (color online). Confidence-level contours in the $\Delta\Gamma_s - \phi_s$ plane for the fit with the Gaussian constraint on the phases δ_1 and δ_2 . The curves correspond to expected CL = 68.3% (dashed) and 90% (solid). The cross shows the best fit point and one-dimensional uncertainties. Also shown is the SM prediction, $\phi_s = -2\beta_s = -0.04$, $\Delta\Gamma_s^{\text{SM}} = 0.088 \pm 0.017$ ps $^{-1}$ [1] and the expected behavior [10] of possible deviations from SM, $\Delta\Gamma_s = \Delta\Gamma_s^{\text{SM}} \cdot |\cos(\phi_s)|$.

interpret the difference between fits with and without this term as a contribution to the systematic uncertainty associated with the background model. The main contributions to systematic uncertainties for the case of free ϕ_s are listed in Table II.

In summary, from a fit to the time-dependent angular distribution of the flavor-tagged decays $B_s^0 \rightarrow J/\psi \phi$, with Gaussian constraint on the strong phases, we have measured the average lifetime of the (B_s^0, \bar{B}_s^0) system, $\bar{\tau}(B_s^0) = 1.52 \pm 0.05 \pm 0.01$ ps, the width difference between the light and heavy B_s^0 eigenstates, $\Delta\Gamma_s = 0.19 \pm 0.07(\text{stat})_{-0.01}^{+0.02}(\text{syst}) \text{ ps}^{-1}$, and the CP -violating phase, $\phi_s = -0.57_{-0.30}^{+0.24}(\text{stat})_{-0.02}^{+0.08}(\text{syst})$. The allowed 90% CL intervals of $\Delta\Gamma_s$ and of ϕ_s are $0.06 < \Delta\Gamma_s < 0.30 \text{ ps}^{-1}$ and $-1.20 < \phi_s < 0.06$. The SM hypothesis for ϕ_s has a P -value of 6.6%.

For the case of free δ_i , no unique parameter values can be reported due to unresolved ambiguities. The allowed ranges of ϕ_s and $\Delta\Gamma_s$ at the 90% CL are $(-1.22 < \phi_s < -0.08, 0.05 < \Delta\Gamma_s < 0.33 \text{ ps}^{-1})$, and $(-3.06 < \phi_s < -1.92, -0.33 < \Delta\Gamma_s < -0.05 \text{ ps}^{-1})$. The SM hypothesis for ϕ_s has a P value of 8.5%. The quoted intervals and P -values do not include the effect of systematic uncertainties, whose impact is nevertheless expected to be negligible. Detailed information on the likelihood variation in the multidimensional parameter space is available elsewhere [16].

The results supersede our previous measurements [4] that were based on the untagged decay $B_s^0 \rightarrow J/\psi \phi$ and a smaller data sample. They are consistent with the recently published CDF results [17].

We thank U. Nierste for useful discussions. We thank the staffs at Fermilab and collaborating institutions, and acknowledge support from the DOE and NSF (USA); CEA and CNRS/IN2P3 (France); FASI, Rosatom and RFBR (Russia); CAPES, CNPq, FAPERJ, FAPESP and FUNDUNESP (Brazil); DAE and DST (India); Colciencias (Colombia); CONACyT (Mexico); KRF and KOSEF (Korea); CONICET and UBACyT (Argentina); FOM (The Netherlands); PPARC (United Kingdom); MSM T (Czech Republic); CRC Program, CFI, NSERC and WestGrid Project (Canada); BMBF and DFG (Germany); SFI (Ireland); The Swedish Research

Council (Sweden); Research Corporation; Alexander von Humboldt Foundation; and the Marie Curie Program.

*Visitor from Augustana College, Sioux Falls, SD, USA.

†Visitor from The University of Liverpool, Liverpool, UK.

‡Visitor from ICN-UNAM, Mexico City, Mexico.

§Visitor from II. Physikalisches Institut, Georg-August-University, Göttingen, Germany.

||Visitor from Helsinki Institute of Physics, Helsinki, Finland.

¶Visitor from Universität Zürich, Zürich, Switzerland.

**Deceased.

- [1] A. Lenz and U. Nierste, J. High Energy Phys. 06 (2007) 072.
- [2] M. Bona *et al.*, J. High Energy Phys. 10 (2006) 081.
- [3] M. Kobayashi and T. Maskawa, Prog. Theor. Phys. **49**, 652 (1973).
- [4] V.M. Abazov *et al.* (D0 Collaboration), Phys. Rev. Lett. **98**, 121801 (2007).
- [5] V.M. Abazov *et al.* (D0 Collaboration), Nucl. Instrum. Methods Phys. Res., Sect. A **565**, 463 (2006).
- [6] V.M. Abazov *et al.* (D0 Collaboration), Phys. Rev. D **76**, 057101 (2007).
- [7] V.M. Abazov *et al.* (D0 Collaboration), Phys. Rev. D **74**, 112002 (2006).
- [8] D0 Collaboration, <http://www-d0.fnal.gov/Run2Physics/WWW/results/prelim/B/B51/>.
- [9] A. S. Dighe, I. Dunietz, and R. Fleischer, Eur. Phys. J. C **6**, 647 (1999).
- [10] I. Dunietz, R. Fleischer, and U. Nierste, Phys. Rev. D **63**, 114015 (2001).
- [11] R. Brun and F. Carminati, CERN Program Library Long Writeup W5013, 1993 (unpublished).
- [12] A. Abulencia *et al.* (CDF Collaboration), Phys. Rev. Lett. **97**, 242003 (2006).
- [13] E. Barberio *et al.* (Heavy Flavor Averaging Group), arXiv:0704.3575
- [14] M. Suzuki, Phys. Rev. D **64**, 117503 (2001).
- [15] B. Aubert *et al.* (BABAR Collaboration), Phys. Rev. D **76**, 031102 (2007).
- [16] D0 Collaboration, <http://www-d0.fnal.gov/Run2Physics/WWW/results/final/B/B08A/>.
- [17] A. Abulencia *et al.* (CDF Collaboration), Phys. Rev. Lett. **100**, 161802 (2008).